**Enerbäck S, Nilsson D, Edwards N, Heglind M, Alkanderi S, Ashton E, Deeb A, Kokash FEB, Bakhsh ARA, Van'tHoff W, Walsh SB, D'Arco F, Daryadel A, Bourgeois S, Wagner CA, Kleta R, Bockenhauer D, Sayer JA. Acidosis and Deafness in Patients with Recessive Mutations in FOXI1. *Journal of the American Society of Nephrology* 2017**

# Acidosis and deafness in patients with recessive mutations in FOXI1

Sven Enerbäck[1,*], M.D., Ph.D., Daniel Nilsson[1], Ph.D., Noel Edwards[2], Ph.D., Mikael Heglind[1], Ph.D., Sumaya Alkanderi[2], M.D., Emma Ashton[3], Ph.D., Asma Deeb[4], M.D., Feras E.B. Kokash[5], M.D., Abdulrahim R.A. Bakhsh[5], William van't Hoff[6], M.D., Stephen B. Walsh[7], M.D., Ph.D., Felice D'Arco[5], M.D., Arezoo Daryadel[8], Ph.D., Soline Bourgeois[8], Ph.D., Carsten A. Wagner[8#], M.D., Robert Kleta[6,7#], M.D., Ph.D., Detlef Bockenhauer[6,7,#], M.D., Ph.D., John Sayer[2,#], M.D., Ph.D.

[1] Department of Medical Biochemistry and Cell Biology, Institute of Biomedicine, University of Gothenburg, SE405 30 Gothenburg, Sweden.

[2] Newcastle University, Institute of Genetic Medicine, Newcastle Upon Tyne, NE1 3BZ, UK.

[3] North East Thames Regional Genetic Service Laboratories, London, UK.

[4] Mafraq Hospital, Abu Dhabi, UAE.

[5] Medical School, Gulf University, Ajman, UAE.

[6] Great Ormond Street Hospital for Children NHS Foundation Trust, London, UK.

[7] UCL Centre for Nephrology, London, UK

[8] Institute of Physiology, University of Zürich, Winterthurerstrasse 190, CH 8057 Zürich, and National Center for Competence in Research NCCR Kidney.CH, Switzerland.

*Corresponding author sven.enerback@medgen.gu.se

#Shared senior authorship

SIGNIFICANCE STATEMENT

Distal renal tubular acidosis (dRTA) is defined by the inability of the distal nephron to acidify the urine and can be associated with sensorineural deafness. About a third of patients with inherited dRTA have no identified causative mutations in known disease genes. Here we report recessive mutations in the forkhead transcription factor FOXI1 as a novel cause of dRTA with deafness. Our findings enable a precise diagnosis in affected patients, inform genetic counselling, as well as cascade screening and provide insight into the transcriptional regulation of transport proteins in the distal nephron and inner ear by FOXI1.

ABSTRACT

Maintenance of the composition of inner ear fluid and regulation of electrolytes and acid-base homeostasis in the collecting duct system of the kidney require an overlapping set of membrane transport proteins, regulated by the forkhead transcription factor FOXI1. In two unrelated consanguineous families, we have identified three patients with previously unknown homozygous missense mutations in *FOXI1* (p.L146F and p.R213P) affecting the highly-conserved DNA-binding domain. Patients presented with early onset sensorineural deafness and distal renal tubular acidosis (dRTA). The mutations reduce DNA-binding affinity of FOXI1, which hence fails to adequately activate genes crucial for normal inner ear function and acid- base regulation in the kidney. A substantial proportion of patients with a clinical diagnosis of inherited dRTA have no identified causative mutations in currently known disease genes. Our data suggest that recessive mutations in FOXI1 can explain the disease in a subset of these patients.

## INTRODUCTION

An important homeostatic function of the kidney is the regulation of acid-base balance. This occurs in the proximal tubule via bicarbonate reabsorption and in the collecting duct system via proton secretion. The intercalated cells of the collecting duct use specific transporters to regulate acid-base balance that can secrete protons (type A intercalated cells) and bicarbonate (type B intercalated cells).[1] Impaired type A intercalated cell function may lead to an inability to acidify the urine and secrete acids, with consequent development of hyperchloremic non-anion gap metabolic acidosis. Mutations known to cause inherited dRTA have been identified in transporters present in the type A intercalated cells and include the B1 and a4 subunits of the vacuolar $H^+$-ATPase (V-ATPase), anion exchanger 1 (AE1) and the cytosolic carbonic anhydrase (CAII).[2-4] Interestingly, mutations in the V-ATPase B1 subunit are typically associated with sensorineural deafness, as can be those in a4,[2,5] emphasizing functional similarities between the epithelium of the inner ear and that of the collecting ducts of the kidney.[6] This is due to the expression of a common set of membrane transport proteins in distinct cell types of the epithelium of the inner ear and the renal collecting duct. Specifically, Forkhead related (FORE) cells of endolymphatic duct and sac epithelium of inner ear[7] and intercalated cells express B1 and a4 subunits of the V-ATPase proton pump and also the anion-exchange protein AE4 and pendrin.[7,8]

A genetic impairment of urine acidification can be associated with an altered pH/ionic composition in the inner ear fluid and hence prevent proper sound perception. Another common feature of these cell types is that they each express *FOXI1* – a transcription factor that has been shown to be crucial for regulation of AE1, AE4, and the V-ATPase subunits B1,

a4, A and E2.[8] Consistent with this, mice with a germline deletion of *Foxi1* display sensorineural deafness and dRTA,[9,10] together with reduced expression of these target genes. Although, a family has been identified, in which Pendred syndrome (PS) segregates with a composite heterozygous genotype of single allele mutations in *SLC26A4* and *FOXI1* (Yang et al.), *y*et, recessive loss-of-function mutations in *FOXI1* have not been described in human patients.

In this report, we describe two novel missense mutations that do not directly affect membrane transport proteins but rather hit cell function at the transcriptional regulatory level – in that they prevent the transcription factor FOXI1 from binding to regulatory DNA cis-elements of target gene promoters. This leads to a severely reduced activation of those target genes, including membrane transport proteins, which require FOXI1 interactions for proper expression. In this way, these two novel loss-of-function mutations induce a severe syndrome of deafness and acidosis with a phenotype very similar to that of mice that altogether lack *Foxi1* expression.

RESULTS AND DISCUSSION

## CASE REPORTS

Two consanguineous kindreds with an autosomal recessive pattern of distal renal tubular acidosis and sensorineural deafness were evaluated (Fig. 1). In family 1, the male proband (Patient 1.1) was the eldest of 3 children, with one affected sister (Patient 1.2; Fig. 1A). In family 2, the female proband (Patient 2.1) was the only affected family member (Fig. 1B). Key clinical features in all affected patients included early onset sensorineural hearing loss requiring cochlear implants, a hypokalemic, hyperchloremic metabolic acidosis at presentation with inappropriately high urine pH, failure-to-thrive, and bilateral nephrocalcinosis (Fig 1E), consistent with dRTA. The deafness was profound and was associated with dilatation of the vestibular aqueduct (Fig. 1F and S3-4). The dRTA was associated with hypercalciuria and nephrocalcinosis noted at presentation, but responded to treatment with both alkali and potassium supplements with subsequent catch-up in growth of the children. In addition, patients 1.1 and 2.1 also developed medullary cystic changes within the kidney (Fig. 1E and 1F). Clinical data are summarized in Table 1.

## STRUCTURAL ANALYSIS OF MUTATED FOXI1 PROTEINS

The novel *FOXI1* homozygous missense mutations, p.L146F and p.R213P, were identified following whole exome sequencing in the affected patients, with segregation of the alleles from the parents (Fig. 1C and 1D). The mutations were not found in the EXaC database. Both missense changes were located within evolutionary highly conserved residues of the FOXI1 protein (Fig. 1G). Consistent with FOX protein sequence alignments (Fig. 1G and Fig. S1), *in*

*silico* modelling of FOXI1, using the crystal structure of rat Foxa3,[11] predicted that FOXI1 L146 occupies a homologous position to L142 in α-helix 2 (α2) of the Foxa3 DNA-binding domain (Fig. 1H and 1I). A stabilizing interaction between Foxa3 and its cognate DNA is formed between the side-chain δ1 carbon atom of L142 and the ribose DNA backbone.[11] Identical results were obtained when modelling FOXI1 on the structures of human FOXM1,[12] human FOXO4,[13] human FOXK2,[14] and rat Foxd3 [15] (Fig. S2), with similar protein-DNA interactions identified for the homologous leucine residues in these structures. The FOXI1 L146F mutation was predicted to disrupt this stabilizing protein-DNA interaction, with the larger (~30Å$^3$),[16] rigid aromatic ring of phenylalanine predicted to impinge upon the ability of the recognition helix (α3) to fully engage the major groove of the target DNA (Fig. 1J). The functional importance of a small hydrophobic residue at this position in the DNA binding domain is highlighted by the almost complete conservation of a leucine residue in the FOX protein family (Fig. S1). FOXI1 R213 was predicted to occupy a homologous position to L209 in the wing 2 domain of Foxa3 (Fig. 1K). Similar to Foxa3 L142, the side-chain β-carbon atom of Foxa3 L209 interacts with the ribose DNA backbone.[11] Therefore, we hypothesized that FOXI1 R213 also served to stabilize the interaction with its target DNA, similar to the role of R210, R211 and R214 in Foxa3 (Fig. 1K). Substitution of the positively charged side-chain of arginine with proline (p.R213P) will destroy the predicted electrostatic interaction with the DNA, thereby disrupting DNA binding (Fig. 1L). (Further modeling information is detailed in the Supplementary Appendix).

**FUNCTIONAL ANALYSIS OF MUTATED FOXI1 PROTEINS**

We further investigated the functional effect of the mutations *in vitro*. First, we assessed protein expression levels of transfected wild type and the mutations p. L146F and p.R213P of FOXI1 in the human kidney cell line HEK 293T, which did not differ (Fig. 2A). Next, we compared trans-activation of wild type and mutant FOXI1, using previously validated promoter constructs,[8,10] for the human a4 subunit of the $H^+$-ATPase (ATP6V0A4), the human anion-exchange protein pendrin (SLC26A4) and the human anion-exchange protein 1 (AE1/SLC4A1). Consistent with our previous data,[8,10] wild type FOXI1 increased reporter gene activity several-fold above empty vector-transfected cells, while the p.L146F or p.R213P mutant constructs show significantly reduced capability to trans-activate these promoters (Fig. 2B). In an electrophoretic mobility shift assay (EMSA) we assessed binding of wild type and mutant FOXI1 proteins to DNA in the form of a canonical FOXI1 binding cis-element. Wild type FOXI1 bound to the oligonucleotide (Fig. 2C, lane 1), whereas no such interaction was detected for the p.L146F or p.R213P mutants (Fig. 2 C, lanes 2 and 3, respectively). Lastly, we used GFP-fusion constructs to determine the intracellular distribution of the wild type and mutant FOXI1 proteins. Distinct nuclear localization was observed for wild type and mutant FOXI1 proteins (Fig. 2D), precluding defective nuclear import as a cause for the reduced trans-activational capacity of the p.L146F and p.R213P mutants. A morphometric analysis of data from figure 2D is shown in figure S5 and an immunochemistry based approach to intracellular localization of FOXI1 and the p.L146F and p.R213P mutants are shown in figure S6. Taken together these experiments show that these mutants have a similar intracellular distribution as wt FOXI1. Our patients with loss-of-function mutations in *FOXI1* recapitulate the phenotype described in a mouse model that

lacks *Foxi1* expression with early onset sensorineural deafness and dRTA.[7,10] The human phenotype we report mimics the renal findings of patients with mutations in the B1 or a4 subunits of the V-ATPase and thus, *FOXI1* mutations are important in the differential diagnosis of dRTA. The phenotypic mimicry is not surprising, considering the previously reported important role of Foxi1 in the regulation of genes associated with dRTA.[3,5,10,17] The discrepancy with respect to the absence or later onset of sensorineural deafness in patients with a4 or, more typically, B1 mutations is likely due to *FOXI1* mutations affecting the regulation of several important membrane transporters, including those critical for inner ear function, whereas isolated impairment of the a4 subunit and B1 accordingly may generate a less severe phenotype that to some extent can be tolerated in the ear. This emphasizes the difference in phenotypic scope between a mutation in a distinct membrane transport protein versus that of a transcription factor that regulates several target genes.

In murine studies, in the intercalated cells of the renal tubules and the FORE cells of the endolymphatic duct and sac of the inner ear, Foxi1 regulates expression of B1 and a4 subunits of the V-ATPase proton pump and also the anion-exchange proteins AE1, AE4, and pendrin. Without expression of a functional Foxi1 protein there is a failure to express these target genes and, as a consequence, this results in severely impaired cellular function, with altered ionic/pH composition of inner ear fluid, and a significantly reduced capacity of the kidneys to secrete an acid load.[9,10] The inner ear phenotype, seen in mice lacking *Foxi1*, is remarkably similar to what we show here for one of the probands (Fig. 1F), with dRTA and an enlargement of the endolymphatic sac and duct resulting in an enlarged vestibular aqueduct syndrome (EVA; Fig. S3 and S4).[7,9]

The biochemical analysis of mutated FOXI1 protein (Fig. 2) demonstrated a severe reduction in the ability to interact with *bona fide* FOXI1 cis-elements with consequent reduced expression of target genes. This is consistent with the *in silico* analysis demonstrating impaired interactions of mutant FOXI1 with the major groove of target DNA (p.L146F) and disturbance of electrostatic interactions with DNA (p.R213P). Together these data demonstrate that, in patients homozygous for these missense *FOXI1* mutations, there is very limited FOXI1 DNA-binding activity, likely resulting in a failure to trans-activate a set of membrane transport proteins needed for normal inner ear and kidney function.

The patients in the present study did not show any signs of goiter, available data on thyroid function was normal. Furthermore, we demonstrate that patients with recessive loss-of-function mutation in FOXI1 display dRTA and deafness with EVA, suggesting that complete loss of FOXI1 activity induces a unique and distinct phenotype. In a previous report, Pendred syndrome associated with a digenic pattern of inheritance in which a composite heterozygous genotype with mutations in *FOXI1* and *SLC26A4* segregates with deafness and an EVA.[18] In this patient goiter was not noted and the contributing missense mutation in *FOXI1* was located approximately 50 amino acids C-terminally of the DNA-binding domain. Also in this report, the authors identify five patients with PS and non-syndromic EVA with a single mutation in one of the *FOXI1* alleles and they speculate that perhaps also single mutations can cause PS and non-syndromic EVA. The apparent lack of a clinical phenotype in the parents of our patients indicates that isolated heterozygous loss of function of FOXI1 does not cause disease, consistent with observations in mice with a heterozygous germ line deletion of Foxi1, who also have no phenotype.[7,9] A similar conclusion was reached in patients with EVA and heterozygous variants in FOXI1, as none had a family history of

deafness.[18] Based on this, we find it unlikely that a single mutation in one *FOXI1* allele will cause disease. However, in combination with another single allele mutation – for instance in a gene that regulate SLC26A4 – a single allele mutation in *FOXI1* could be part of the pathogenetic mechanism underlying PS with non-syndromic EVA.

Of interest, in mice lacking *Foxi1*, males have been shown to be infertile.[19] This is due to a failure of clear cells in the epididymis to acidify the extracellular luminal fluid. This leads to a pathological post-testicular sperm maturation and, as a consequence, spermatozoa from *Foxi1* null males fail to reach the female genital tract in sufficient number to allow fertilization.[19] Whether mutations in *FOXI1* will be associated with reduced male fertility also in man remains an open question as for the one male patient in our study analysis of spermatozoa function was not available. FOXI1 is highly expressed in human renal kidney cortex (RNA-Seq expression data from GTEx https://www.gtexportal.org). Other human tissues which express FOXI1 at more modest levels include breast tissue, salivary gland, prostate and skin (https://www.gtexportal.org/home/gene/ENSG00000168269.7). The human protein atlas reveals high levels of FOXI1 protein expression in kidney, and low expression levels in nasopharynx, bronchus, salivary gland and breast tissue (https://www.proteinatlas.org/ENSG00000168269-FOXI1/tissue). Thus, it is possible that other tissues/cell types than those reported here display pathological phenotypes in response to loss-of-function mutations in FOXI1.

All three patients in this study were noted to have medullary renal cysts, raising the question whether FOXI1 could also be involved in cystogenesis. Yet, an association of dRTA with cysts is well recognized: in our own cohort of children with dRTA, over a third developed cysts

during childhood.[20] Typically, this is ascribed to hypokalemia,[21] although other factors, such as hypercalciuria/nephrocalcinosis have also been implicated.[22] Observations in more patients with dRTA are needed to better assess the frequency of cysts in FOXI1-based dRTA compared to other genetic forms.

Approximately a third of patients with dRTA have no identified causative mutation in recognized disease genes,[20,23,24] and thus should be tested for *FOXI1* mutations to help establish a precise diagnosis with consequent genetic counseling – especially in cases involving hearing and possibly also male fertility problems.[19]

## METHODS

This study was approved by the respective institutional review boards (Institute of Child Health/Great Ormond Street Hospital Research Ethics Committee 05/Q0508/6; Newcastle and North Tyneside Research Ethics Committee 2003/163).

Parents provided written informed consent. Three subjects with dRTA and sensorineural deafness, without identified mutations in known disease genes were investigated. We performed whole exome sequencing using peripheral blood DNA from affected family members. Sanger sequencing was used to validate the variants identified by whole exome sequencing in both affected children. *In silico* modelling and biochemical analysis was performed with human FOXI1 protein as a control compared with the two mutated FOXI1 proteins.

### Whole-exome sequencing and identification of *FOXI1* sequence variant

#### *Exome capture and Next-Generation sequencing*

Whole exome sequencing of affected Patients 1.1 and 1.2 was performed by GATC Biotech using the Illumina HiSeq-2000 (Illumina Inc., San Diego, CA). The genomic DNA was captured on the SureSelectXT Human All Exon V5 kit (Agilent, CA) to capture target sequence of exonic regions and non-coding RNAs in the human genome. The paired-end Illumina libraries were captured in solution according to the Agilent SureSelect protocol with 125 bp read length. Perkin Elmer (UK) provided commercially available exome sequencing for Patient 2.1 (Exome capture Agilent SureSelect V4; Read Length / Library construction: 75-100bp/paired

end library and reads; Sequence Coverage: ~35X mean coverage; Detection of sequencing fragments via the Illumina Hiseq2000).

*SNP detection*

The base quality of each sequence read was inspected for low quality calls and subsequently removed before proceeding with further processing. Using a sliding window approach, bases with low quality were removed from the 3' and 5' ends. Bases were removed if the average quality was below the threshold of 15. Finally, only reads with both forward, and reverse read, were used for the next analysis step. Mapping to the reference database (hg19, NCBI37) was performed using Burrows-Wheeler Alignment (BWA) method with default parameters. The SNP and Indel calling was performed using GATK's UnifiedGenotyper using a Bayesian genotype likelihood model to estimate simultaneously the most likely genotypes and allele frequency in a population of N samples. Variants detected were annotated based on their gene context using snpEff. The total reads were ~145M with the percentage of mapped reads 99%. Data was pipelined to allow Indel and SNP vcf files to be generated which were viewed using Ingenuity Variant Analysis software (Qiagen).

**Filtering criteria used for single nucleotide variants (SNVs), and insertion and deletion selection (Indel).**

| | Family 1 (1.1 and 1.2) | Family 2 (2.1) |
|---|---|---|
| Number of variants | 176834 | 80397 |
| Variants of high confidence | 158256 | 79590 |
| SNVs/Indel ≤ 1% in HapMap18 and 1000 Genome database | 14363 | 6190 |

| | | |
|---|---|---|
| Predicted deleterious | 1076 | 2347 |
| Biological context (kidney disease, renal tubular acidosis) | 217 | 8 |
| Present on both alleles in all affected individuals* | 1 | 1 |

*Affected members after screening of kindred based on clinical and biochemical features.

**PCR primers used for Sanger sequencing**

| | | | |
|---|---|---|---|
| FOXI1 | FWD | CAACCCCTACCTCTGGTTCA | Exon 1 |
| FOXI1 | REV | GGGGAGGAAGGAAGTGAGTC | Exon 1 |
| FOXI1 | FWD | CATCTGTCACCTTGGCTTT | Exon 2 |
| FOXI1 | REV | GGGGAGAAGGAGTTGAAGGT | Exon 2 |

For experimental details regarding *in silico* modelling and cell-based experiments see Supplementary Appendix.

AUTHOR CONTRIBUTIONS

DN, NE, MH, AD, SB, CAW, SE performed in vitro experiments; WvH, SBW, FD, FEBK, ARAB, SA, EA, RK, DB, JAS executed genetic analysis and collection of families; SE, CAW, RK, DB, JAS wrote the manuscript.

ACKNOWLEDGEMENTS

See Supplementary Appendix.

REFERENCES


1. Wagner CA, Devuyst O, Bourgeois S, Mohebbi N. Regulated acid-base transport in the collecting duct. Pflugers Archiv : European journal of physiology 2009;458:137-56.
2. Karet FE, Finberg KE, Nelson RD, et al. Mutations in the gene encoding B1 subunit of H+-ATPase cause renal tubular acidosis with sensorineural deafness. Nature genetics 1999;21:84-90.
3. Smith AN, Skaug J, Choate KA, et al. Mutations in ATP6N1B, encoding a new kidney vacuolar proton pump 116-kD subunit, cause recessive distal renal tubular acidosis with preserved hearing. Nature genetics 2000;26:71-5.
4. Sly WS, Whyte MP, Sundaram V, et al. Carbonic anhydrase II deficiency in 12 families with the autosomal recessive syndrome of osteopetrosis with renal tubular acidosis and cerebral calcification. The New England journal of medicine 1985;313:139-45.
5. Stover EH, Borthwick KJ, Bavalia C, et al. Novel ATP6V1B1 and ATP6V0A4 mutations in autosomal recessive distal renal tubular acidosis with new evidence for hearing loss. Journal of medical genetics 2002;39:796-803.
6. Stankovic KM, Brown D, Alper SL, Adams JC. Localization of pH regulating proteins H+ATPase and Cl-/HCO3- exchanger in the guinea pig inner ear. Hearing research 1997;114:21-34.
7. Hulander M, Kiernan AE, Blomqvist SR, et al. Lack of pendrin expression leads to deafness and expansion of the endolymphatic compartment in inner ears of Foxi1 null mutant mice. Development 2003;130:2013-25.
8. Vidarsson H, Westergren R, Heglind M, Blomqvist SR, Breton S, Enerback S. The forkhead transcription factor Foxi1 is a master regulator of vacuolar H-ATPase proton pump subunits in the inner ear, kidney and epididymis. PloS one 2009;4:e4471.
9. Hulander M, Wurst W, Carlsson P, Enerback S. The winged helix transcription factor Fkh10 is required for normal development of the inner ear. Nature genetics 1998;20:374-6.
10. Blomqvist SR, Vidarsson H, Fitzgerald S, et al. Distal renal tubular acidosis in mice that lack the forkhead transcription factor Foxi1. The Journal of clinical investigation 2004;113:1560-70.
11. Clark KL, Halay ED, Lai E, Burley SK. Co-crystal structure of the HNF-3/fork head DNA-recognition motif resembles histone H5. Nature 1993;364:412-20.
12. Littler DR, Alvarez-Fernandez M, Stein A, et al. Structure of the FoxM1 DNA-recognition domain bound to a promoter sequence. Nucleic acids research 2010;38:4527-38.
13. Boura E, Rezabkova L, Brynda J, Obsilova V, Obsil T. Structure of the human FOXO4-DBD-DNA complex at 1.9 A resolution reveals new details of FOXO binding to the DNA. Acta crystallographica Section D, Biological crystallography 2010;66:1351-7.
14. Tsai KL, Huang CY, Chang CH, Sun YJ, Chuang WJ, Hsiao CD. Crystal structure of the human FOXK1a-DNA complex and its implications on the diverse binding specificity of winged helix/forkhead proteins. The Journal of biological chemistry 2006;281:17400-9.
15. Jin C, Marsden I, Chen X, Liao X. Dynamic DNA contacts observed in the NMR structure of winged helix protein-DNA complex. Journal of molecular biology 1999;289:683-90.
16. Tsai J, Taylor R, Chothia C, Gerstein M. The packing density in proteins: standard radii and volumes. Journal of molecular biology 1999;290:253-66.
17. Bruce LJ, Cope DL, Jones GK, et al. Familial distal renal tubular acidosis is associated with mutations in the red cell anion exchanger (Band 3, AE1) gene. The Journal of clinical investigation 1997;100:1693-707.
18. Yang T, Vidarsson H, Rodrigo-Blomqvist S, Rosengren SS, Enerback S, Smith RJ. Transcriptional control of SLC26A4 is involved in Pendred syndrome and nonsyndromic enlargement of vestibular aqueduct (DFNB4). American journal of human genetics 2007;80:1055-63.
19. Blomqvist SR, Vidarsson H, Soder O, Enerback S. Epididymal expression of the forkhead transcription factor Foxi1 is required for male fertility. The EMBO journal 2006;25:4131-41.

20. Besouw MTP, Bienias M, Walsh P, et al. Clinical and molecular aspects of distal renal tubular acidosis in children. Pediatric nephrology 2017;32:987-96.
21. Alpern RJ, Toto RD. Hypokalemic nephropathy--a clue to cystogenesis? The New England journal of medicine 1990;322:398-9.
22. Walsh SB, Unwin E, Vargas-Poussou R, Houillier P, Unwin R. Does hypokalaemia cause nephropathy? An observational study of renal function in patients with Bartter or Gitelman syndrome. QJM : monthly journal of the Association of Physicians 2011;104:939-44.
23. Palazzo V, Provenzano A, Becherucci F, et al. The genetic and clinical spectrum of a large cohort of patients with distal renal tubular acidosis. Kidney international 2017;91:1243-55.
24. Ashton E, Legrand A, Benoit V, et al. Simultaneous sequencing of 37 genes identifies likely causative mutations in the majority of children with renal tubulopathies. Kidney international 2017;In Press.

Table 1: Clinical and genetic characteristics of affected patients

| **Patient ID** | **1.1**[*] | **1.2**[*] | **2.1**[†] |
|---|---|---|---|
| **Sex** | Male | Female | Female |
| **Ethnicity** | UAE[‡] | UAE[‡] | Iraq |
| **Mutation**[§] | | | |
| **Nucleotide** | c.436C>T | c.436C>T | c.638G>C |
| **Amino acid substitution** | p.Leu146Phe | p.Leu146Phe | p.Arg213Pro |
| **Allele frequency** | Not present in EXaC[‖] | Not present in EXaC[‖] | Not present in EXaC[‖] |
| **dRTA presentation** | | | |
| Age at diagnosis [years] | 8 | 6 | <1 |
| Symptoms | Rickets | Rickets | Failure-to-thrive, rickets |
| Weight [kg] (SDS[¶]) | 18 (-2.9) | 16 (-1.9) | 9 (-3.5) |
| Height [cm] (SDS[¶]) | 119 (-1.6) | 105 (-2.0) | 83.5 (-2.5) |
| **Blood biochemistries** | | | |
| pH | 7.30 | 7.30 | 7.30 |
| tCO2 [mmol/l] | 16 | 17 | 14 |
| Potassium [mmol/l] | 3.6 | 3.4 | 3.5 |
| Estimated GFR [ml/min/1.73m$^2$] | 87 | 99 | 110 |
| **Urine biochemistries** | | | |
| pH | 8 | 8 | 8 |
| Calcium/creatinine ratio [mmol/mmol] (upper limit of normal) | 0.20 (<0.6)[**] | 0.26 (<1.1)[**] | 4.25 (<1.4) |
| **Radiology** | | | |
| Nephrocalcinosis (age detected) [††] | yes (10 years) | yes (9 years) | yes (2 years) |
| Medullary cysts (age detected) | yes (10 years) | yes (9 years) | yes (8 years) |
| **Deafness** | | | |
| Age at diagnosis [years] | 1 | 1 | 2 |
| Cochlear implant (age inserted) | yes (4 years) | yes (4 years) | yes (13 years) |

*Data at presentation for patient 1.1 and 1.2 are from first presentation in tertiary center in UAE aged 8 and 6 years respectively.

†Data at presentation for patient 2.1 are from first presentation in the UK age 2 years, when she was partially treated. Data from the initial presentations are not available.

‡ UAE: United Arab Emirates

§ Mutations were homozygous in all 3 patients

‖ EXaC: Exome Aggregation Consortium

¶ SDS: Standard deviation score

**Urine calcium/creatinine values pre-treatment are unavailable, normocalciuria was seen in the context of correction of metabolic acidosis.
†† The first renal imaging of patients 1.1 and 1.2 was at age 10 and 9 years, respectively. Nephrocalcinosis and cysts may have been present earlier.

**Figure 1**

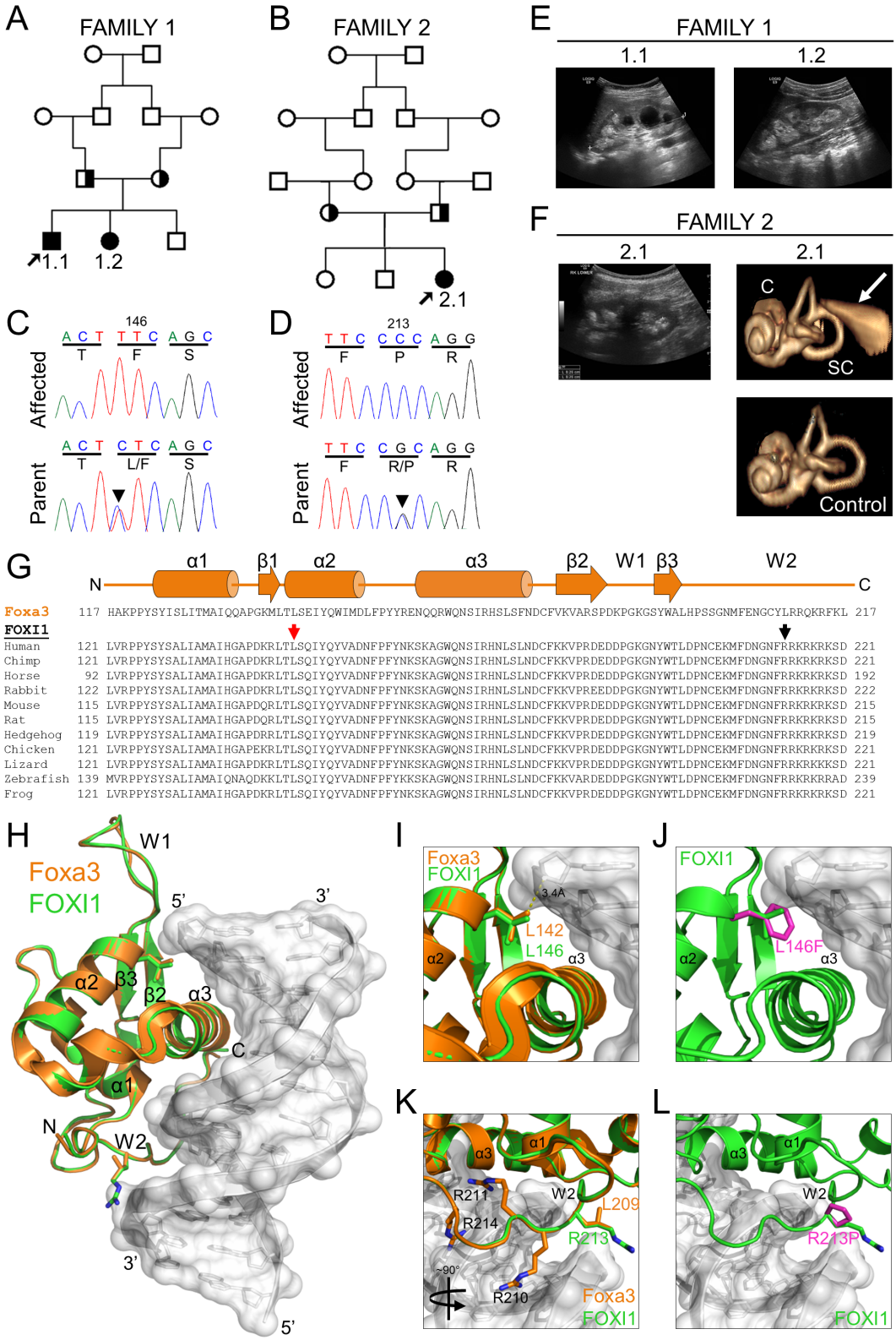
A
FAMILY 1
1.1
1.2
B
FAMILY 2
2.1
C
146
A C T T T C A G C
T F S
Affected
A C T C T C A G C
T L/F S
Parent
D
213
T T C C C C A G G
F P R
Affected
T T C C G C A G G
F R/P R
Parent
E
FAMILY 1
1.1
1.2
F
FAMILY 2
2.1
2.1
C
SC
Control
G
α1 β1 α2 α3 β2 W1 β3 W2
N C
Foxa3 117 HAKPPYSYISLITMAIQQAPGKMLTLSEIYQWIMDLFPYYRENQQRWQNSIRHSLSFNDCFVKVARSPDKPGKGSYWALHPSSGNMFENGCYLRRQKRFKL 217
FOXI1
Human 121 LVRPPYSYSALIAMAIHGAPDKRLTLSQIYQYVADNFPFYNKSKAGWQNSIRHNLSLNDCFKKVPRDEDDPGKGNYWTLDPNCEKMFDNGNFRRKRKRKSD 221
Chimp 121 LVRPPYSYSALIAMAIHGAPDKRLTLSQIYQYVADNFPFYNKSKAGWQNSIRHNLSLNDCFKKVPRDEDDPGKGNYWTLDPNCEKMFDNGNFRRKRKRKSD 221
Horse 92 LVRPPYSYSALIAMAIHGAPDKRLTLSQIYQYVADNFPFYNKSKAGWQNSIRHNLSLNDCFKKVPRDEDDPGKGNYWTLDPNCEKMFDNGNFRRKRKRKSD 192
Rabbit 122 LVRPPYSYSALIAMAIHGAPDKRLTLSQIYQYVADNFPFYNKSKAGWQNSIRHNLSLNDCFKKVPREEDDPGKGNYWTLDPNCEKMFDNGNFRRKRKRKSD 222
Mouse 115 LVRPPYSYSALIAMAIHGAPDQRLTLSQIYQYVADNFPFYNKSKAGWQNSIRHNLSLNDCFKKVPRDEDDPGKGNYWTLDPNCEKMFDNGNFRRKRKRKSD 215
Rat 115 LVRPPYSYSALIAMAIHGAPDQRLTLSQIYQYVADNFPFYNKSKAGWQNSIRHNLSLNDCFKKVPRDEDDPGKGNYWTLDPNCEKMFDNGNFRRKRKRKSD 215
Hedgehog 119 LVRPPYSYSALIAMAIHGAPDRRLTLSQIYQYVADNFPFYNKSKAGWQNSIRHNLSLNDCFKKVPRDEDDPGKGNYWTLDPNCEKMFDNGNFRRKRKRKSD 219
Chicken 121 LVRPPYSYSALIAMAIHGAPEKRLTLSQIYQYVADNFPFYNKSKAGWQNSIRHNLSLNDCFKKVPRDEDDPGKGNYWTLDPNCEKMFDNGNFRRKRKRKSD 221
Lizard 121 LVRPPYSYSALIAMAIHGAPDKRLTLSQIYQYVADNFPFYNKSKAGWQNSIRHNLSLNDCFKKVPRDEDDPGKGNYWTLDPNCEKMFDNGNFRRKRKKKSD 221
Zebrafish 139 MVRPPYSYSALIAMAIQNAQDKKLTLSQIYQYVADNFPFYKKSKAGWQNSIRHNLSLNDCFKKVARDEDDPGKGNYWTLDPNCEKMFDNGNFRRKRKRRAD 239
Frog 121 LVRPPYSYSALIAMAIHGAPDKRLTLSQIYQYVADNFPFYNKSKAGWQNSIRHNLSLNDCFKKVPRDEDDPGKGNYWTLDPNCEKMFDNGNFRRKRKRKSD 221
H
W1
Foxa3
FOXI1
5'
3'
α2
β3
β2
α3
C
α1
N
W2
3'
5'
I
Foxa3
FOXI1
3.4Å
L142
L146
α2
α3
J
FOXI1
L146F
α2
α3
K
α3
α1
R211
W2
L209
R214
R213
~90°
R210
Foxa3
FOXI1
L
α3
α1
W2
R213P
FOXI1

**Figure 2**

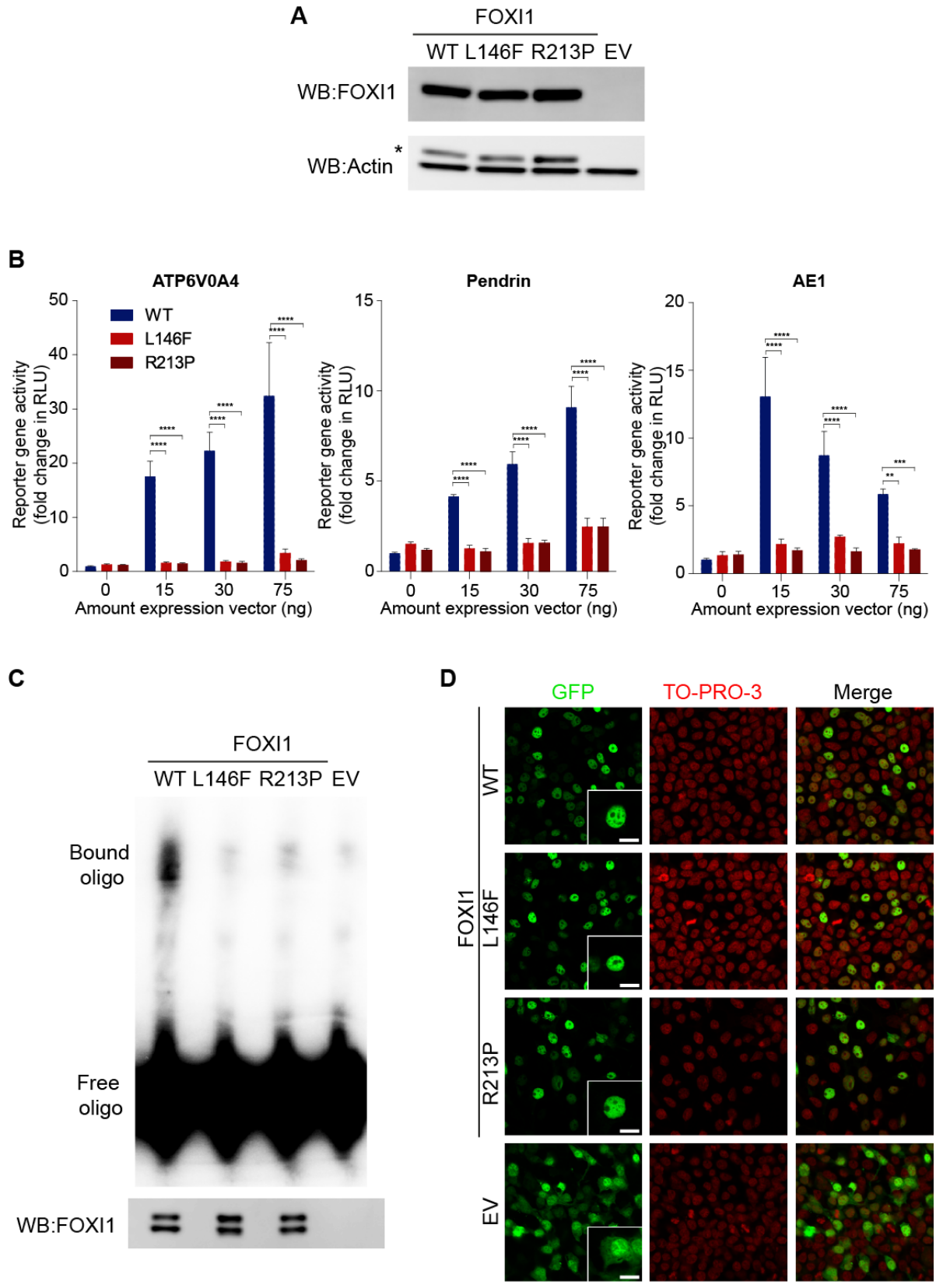
A
FOXI1
WT L146F R213P EV
WB:FOXI1
WB:Actin *
B
ATP6V0A4
Pendrin
AE1
WT
L146F
R213P
Reporter gene activity (fold change in RLU)
Amount expression vector (ng)
0
15
30
75
C
FOXI1
WT L146F R213P EV
Bound oligo
Free oligo
WB:FOXI1
D
GFP
TO-PRO-3
Merge
FOXI1
WT
L146F
R213P
EV

FIGURE LEGENDS

**Figure 1.** Panel A and B shows the family pedigrees and status with respect to *FOXI1* mutation genotype. Squares denote male family members, circles female members. Shaded symbols denote affected members with homozygous mutation, semi-shaded symbols denote heterozygous carriers. Arrows denote the probands (Patient 1.1 in Family 1 and Patient 2.1 in Family 2). Panel C and D show sequence chromatograms of the affected and parental genotype. Mutations are marked with an arrowhead. Panels E and F show renal ultrasound scans demonstrating medullary nephrocalcinosis in all affected and cystic change within the kidneys in Patient 1.1 and 2.1. CT volumetric rendering of the right labyrinth in Patient 2.1 revealed dilation of the endolymphatic sac (panel F, white arrow) compared with healthy control (panel F, lower CT scan). Note the normal appearance of the cochlea (C) and lateral semicircular canals (SC) in Patient 2.1. Panel G depicts the secondary structural elements of the Foxa3 DNA-binding domain (α-helices, cylinders; β-sheets, arrows; and wing domains, W1 and W2) above sequence alignments with FOXI1 proteins from various species. FOXI1 L146 in helix 2 (α2) is indicated by the red arrow, and FOXI1 R213 in wing 2 (W2) by the black arrow. Panel H shows superposition of the human FOXI1 homology model (in green) with the crystal structure of Foxa3 (in orange) bound to DNA. The recognition helix (α3) of Foxa3 is positioned in the major groove of the cognate DNA and stabilized in part by a 3.4Å interaction between Foxa3 L142 and the sugar-phosphate backbone (Panel I). Mutation of the homologous leucine residue in FOXI1 to phenylalanine (L146F; colored magenta, panel J) is predicted to disrupt DNA binding. Panel K shows a close-up view of the wing 2 domain (W2) of Foxa3 and FOXI1. L209 in Foxa3 forms a 4.3Å interaction with the DNA backbone. The structurally homologous FOXI1 R213 is predicted to facilitate DNA binding, similar to the role of R210, R211 and R214 in W2 of Foxa3. Mutation of FOXI1 R213 to proline (R213P; colored magenta, panel L) will destroy the electrostatic interaction with DNA.

**Figure 2.** Effect of *FOXI1* mutations on protein stability, promoter transactivation, DNA binding and cellular localization. Western blot analysis of FOXI1 protein expression (Panel A) in whole cell lysates from HEK 293T cells transfected with FOXI1 wild type (WT), L146F mutant, R213P mutant, or empty vector (EV). To determine equal protein loading, the membrane was stripped and re-probed for β-actin. * indicates incomplete stripping of signal from the FOXI1 labelling. Panel B demonstrates reporter gene activity, expressed in relative luciferase units (RLU), upon co-transfection of increasing amounts (15, 30 and 75 ng) of FOXI1 expression plasmid and 25 ng of ATP6V0A4, pendrin, or AE1 promoter reporter constructs in HEK 293T cells. Level of significance, calculated by two-way ANOVA using GraphPad Prism 5, is indicated; ** $p < 0,01$, *** $p < 0,001$. **** $p < 0,0001$. Panel C shows EMSA using in vitro transcribed/translated FOXI1 wild type (WT), L146F, or R213P, and empty vector (EV) as control, and radio-labelled oligonucleotides harboring a FOXI1 binding site. Bound and unbound oligonucleotides (oligos) are marked. Lower panel shows a Western blot of the transcribed/translated products. Panel D illustrates the intracellular localization of FOXI1-GFP fusion proteins after transfection of HEK 293T cells with FOXI1 wild type, L146F, or R213P mutants, or empty vector (EV) respectively. Green channel; GFP signal (inset shows zoom in on single cell), red channel; nuclear staining (TO-PRO-3), and merge channel; all channels together. Scale bar is 10 μm.

# SUPPLEMENTARY APPENDIX

## *In silico* modelling

The DNA-binding domain (residues 121-221) of human FOXI1 (accession number NP_036320) was modelled against the crystal structure of rat Foxa3 (hepatocyte nuclear factor-3γ/HNF-3γ)) (PDB accession code 1VTN)[1] using HHPred[2] and Modeller[3] software. Homology model figures were prepared using PyMOL (http://www.pymol.org/). Consistent with protein sequence alignments (Fig. S1), identical results were obtained using the crystal structures of FOXM1,[4] FOXO4,[5] FOXK2,[6] and Foxd3[7] (Fig. S2). It should be noted that predicted position of the FOXI1 R213 residue was specific to the Foxa3 homology model since this region of the wing 2 domain in the other structures used for modelling was either not resolved or captured in contact with the DNA. Interestingly, a similar missense mutation (p.R169P) in FOXC1 has been shown to disrupt DNA binding and transcriptional activation.[8] Sequence analysis predicts FOXC1 R169 occupies a homologous position to FOXI1 R214, just one residue downstream of FOXI R213 (Fig. S1), thereby providing further evidence for the functional importance of this domain.

## Plasmid constructs

Full length FOXI1 coding sequence was previously cloned into the expression vector pcDNA3.1.[9] FOXI1 was also cloned in-frame with GFP in the expression vector pEGFP-N3 (Clontech, USA), to make FOXI1-GFP fusion protein. Mutant FOXI1 L146F and R213P were generated by site-directed mutagenesis using Quikchange Lightning Site-directed mutagenesis kit (Agilent Technologies, USA) using the following primers (mutations underlined):

FOXI1 p.L146F FWD 5'-ATCTGGCTGAAAGTGAGGCGCTTGTCGGGT-3';

FOXI1 p.L146F REV 5'-ACCCGACAAGCGCCTCACTTTCAGCCAGAT-3';

FOXI1 p.R213P FWD 5'-ATTTTCTCTTCCTTTTCCTGGGGAAATTTCCATTGTCGAAC-3';

FOXI1 p.R213P REV 5'-GTTCGACAATGGAAATTTCCCCAGGAAAAGGAAGAGAAAAT-3'

Promoter reporter constructs were previously generated by cloning promoter regions of ATP6V0A4,[10] AE1 (SLC4A1),[9] and pendrin (SLC26A4) [9] into pGL3 Basic vector (Promega, USA). The sequence of each construct was verified by Sanger sequencing performed by GATC Biotech Ltd (Germany).

### Cell culture, transfections, and luciferase assay

Human embryonic kidney (HEK) cell line 293T (ATCC® CRL-3216™) was maintained on gelatin coated flasks in Dulbecco's Modified Eagle medium (DMEM, Thermo Fisher Scientific, USA; 41965-039) supplemented with 10% fetal bovine serum (Thermo Fisher Scientific, USA; 16140-071) and 1 mM sodium pyruvate (Thermo Fisher Scientific, USA; 11360-039). Transient transfections were performed using Lipofectamine 2000 transfection reagent (Thermo Fisher Scientific, USA; 11668-019) according to manufacturer's protocol.

For luciferase assays, cells 90-100% confluence were trypsinized, added to a DNA/Lipofectamine mix in Opti-MEM® I Reduced Serum Medium (Thermo Fisher Scientific, USA; 31985-070) and then plated, in triplicate, with dilution approximately 1:1, into gelatin coated 96-well plates (Sarstedt, Germany; 83.1835.300). Cells were co-transfected with 0, 15, 30 or 75 ng of FOXI1 expression plasmid and 25 ng of the luciferase promoter constructs for ATP6V0A4, AE1 (SLC4A1) or pendrin (SLC26A4). Renilla luciferase plasmid (20 pg) pRL-SV40 (Promega, USA; E2231) was used to control for transfection efficiency. Empty pcDNA3.1 plasmid was used to equalize the total amount of DNA added to 100 ng/well.

Two days after transfection cells were assayed using Dual-Luciferase® Reporter Assay System (Promega, USA; E1910) according to manufacturer's protocol. Briefly, culture medium was removed and 25 µl of Passive Lysis Buffer was added to each well. Cells were then incubated at room temperature with slow rocking for 30 minutes where after 20 µl of lysate from each well was transferred to corresponding wells of a white 96-well plate (Greiner, Austria; Cat. No.: 655075) for the analysis, which was performed on a Tecan infinite M200 plate reader. Results were calculated as the quotient between values for luciferase and values for Renilla luciferase, all normalized to values for 0 ng FOXI1 expression plasmid. For intracellular distribution analysis HEK 293T cells, seeded in 24-well plates on gelatin-coated glass coverslips, were transfected with 500 ng/well of pEGFP-N3 plasmids containing wild type, L146F or R213P FOXI1 or no insert (empty vector). Two days after transfection, cells were fixed for 15 min in 4% paraformaldehyde in PBS, permeabilized in 0.1% Triton X-100 in PBS for 5 min and incubated at room temperature for 30 min with fluorescent nuclear marker TO-PRO-3 (Thermo Fisher Scientific, USA; T3605). After subsequent washes in PBS, coverslips were mounted with ProLong Diamond Antifade Mountant (Thermo Fisher Scientific, USA; P36961). Imaging of GFP and TO-PRO-3 signals was performed using a Zeiss LSM500 Meta system.

### Western blot

HEK 293T cells were lysed in RIPA buffer (50 mM Tris-HCl, pH 8.0, 1 mM EDTA, 1% NP-40, 0.1% sodium deoxycholate, 0.1% SDS, 150 mM NaCl), supplemented with cOmplete™, EDTA-free Protease Inhibitor Cocktail (Roche, Switzerland) according to the manufacturer's recommendations. Proteins, from either cell lysates or *in vitro* translation/transcription, were separated by SDS-PAGE on NuPAGE Novex 4-12% Bis-Tris protein gels (Thermo Fisher

Scientific, USA) and transferred to PVDF membrane (Millipore, USA). FOXI1 protein was detected with polyclonal goat antibody (ab20454, Abcam, UK) diluted 1:500 in blocking buffer (5% (w/v) skim milk powder, 50 mM Tris-Cl, pH 7.5, 150 mM NaCl, 0.02% (v/v) Tween20) followed by horseradish peroxidase (HRP)-coupled polyclonal rabbit anti-goat IgG (Dako, Denmark) diluted 1:2000 in blocking buffer. HRP-coupled β-actin monoclonal mouse antibody (ab20272, Abcam, UK), diluted 1:5000 in blocking buffer, was used as a loading control of cell lysates. HRP-coupled antibody was visualized with SuperSignal West Dura Chemiluminescent Substrates (Thermo Fisher Scientific, USA) on a LAS-4000 Luminescent Image analyzer (FujiFilm, Japan).

## Electrophoretic mobility shift assay (EMSA)

*In vitro* transcription/translations were performed according to the manufacturer's protocol using TNT® T7 Quick Coupled Transcription/Translation System (Promega, USA) and 1 µg expression plasmid. Oligonucleotides, previously shown to have binding affinity for wild type FOXI1 protein,[11] were annealed and labeled using Klenow polymerase (Roche, Switzerland) and [α-$^{32}$P]dCTP (PerkinElmer, USA). For each binding reaction 400000 CPM of labeled probe was incubated with 3 µl of *in vitro* translated FOXI1 protein and 1 µg of poly dI:dC in binding buffer (5 mM HEPES, 23% glycerol, 1.5 mM MgCl2, 0.2 mM EDTA, 0.5 mM DTT, 100 mM KCl) supplemented with cOmplete™, EDTA-free Protease Inhibitor Cocktail (Roche, Switzerland) at room temperature for 30 min. To the reactions Native Tris-Glycine Sample buffer (2X) was added and samples were resolved on Novex™ 6% Tris-Glycine Mini Gel and run the gel at 125 V in Novex™ Tris-Glycine Native Running Buffer (Thermo Fisher Scientific, USA). After electrophoresis, the gel was dried using a Gel Dryer Model 583 (Bio-Rad, USA), in combination with HydroTech Vacuum Pump (Bio-Rad, USA), for 2 h at 80° C and exposed to

BAS image plate (FujiFilm, Japan). The BAS image plate was subsequently scanned using FLA-7000 scanner (FujiFilm, Japan).

SUPPLEMENTARY FIGURES

**Figure S1.**

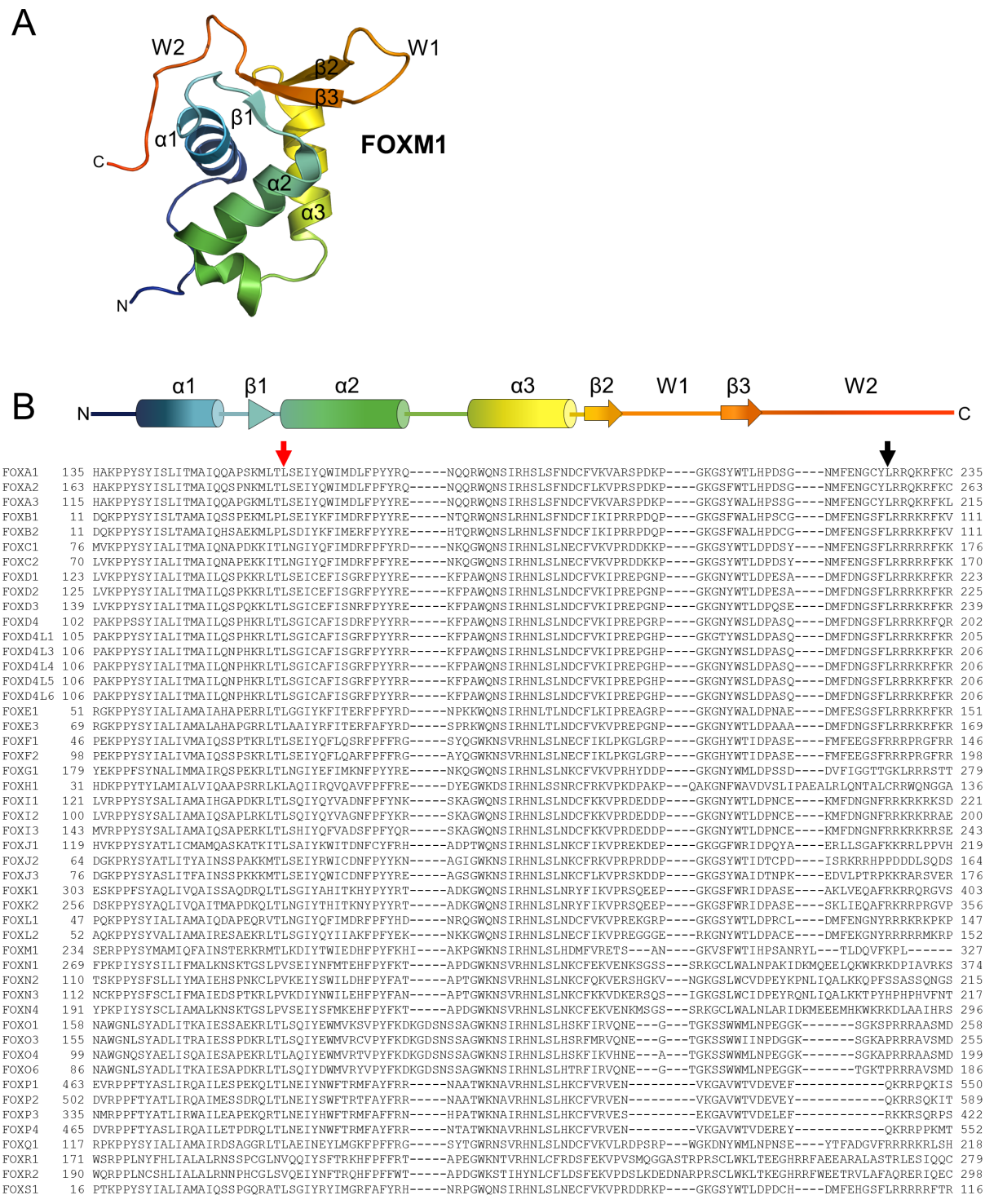


```
FOXA1   135 HAKPPYSYISLITMAIQQAPSKMLTLSEIYQWIMDLFPYYRQ-----NQQRWQNSIRHSLSFNDCFVKVARSPDKP----GKGSYWTLHPDSG----NMFENGCYLRRQKRFKC 235
FOXA2   163 HAKPPYSYISLITMAIQQSPNKMLTLSEIYQWIMDLFPFYRQ-----NQQRWQNSIRHSLSFNDCFLKVPRSPDKP----GKGSFWTLHPDSG----NMFENGCYLRRQKRFKC 263
FOXA3   115 HAKPPYSYISLITMAIQQAPGKMLTLSEIYQWIMDLFPYYRE-----NQQRWQNSIRHSLSFNDCFVKVARSPDKP----GKGSYWALHPSSG----NMFENGCYLRRQKRFKL 215
FOXB1    11 DQKPPYSYISLTAMAIQSSPEKMLPLSEIYKFIMDRFPYYRE-----NTQRWQNSLRHNLSFNDCFIKIPRRPDQP----GKGSFWALHPDCG----DMFENGSFLRRRKRFKV 111
FOXB2    11 DQKPPYSYISLTAMAIQHSAEKMLPLSDIYKFIMERFPYYRE-----HTQRWQNSLRHNLSFNDCFIKIPRRPDQP----GKGSFWALHPDCG----DMFENGSFLRRRKRFKV 111
FOXC1    76 MVKPPYSYIALITMAIQNAPDKKITLNGIYQFIMDRFPFYRD-----NKQGWQNSIRHNLSLNECFVKVPRDDKKP----GKGSYWTLDPDSY----NMFENGSFLRRRRFKK 176
FOXC2    70 LVKPPYSYIALITMAIQNAPEKKITLNGIYQFIMDRFPFYRE-----NKQGWQNSIRHNLSLNECFVKVPRDDKKP----GKGSYWTLDPDSY----NMFENGSFLRRRRFKK 170
FOXD1   123 LVKPPYSYIALITMAILQSPKKRLTLSEICEFISGRFPYYRE-----KFPAWQNSIRHNLSLNDCFVKIPREPGNP----GKGNYWTLDPESA----DMFDNGSFLRRRKRFKR 223
FOXD2   125 LVKPPYSYIALITMAILQSPKKRLTLSEICEFISGRFPYYRE-----KFPAWQNSIRHNLSLNDCFVKIPREPGNP----GKGNYWTLDPESA----DMFDNGSFLRRRKRFKR 225
FOXD3   139 LVKPPYSYIALITMAILQSPQKKLTLSGICEFISNRFPYYRE-----KFPAWQNSIRHNLSLNDCFVKIPREPGNP----GKGNYWTLDPQSE----DMFDNGSFLRRRKRFKR 239
FOXD4   102 PAKPPSSYIALITMAILQSPHKRLTLSGICAFISDRFPYYRR-----KFPAWQNSIRHNLSLNDCFVKIPREPGRP----GKGNYWSLDPASQ----DMFDNGSFLRRRKRFQR 202
FOXD4L1 105 PAKPPYSYIALITMAILQSPHKRLTLSGICAFISGRFPYYRR-----KFPAWQNSIRHNLSLNDCFVKIPREPGHP----GKGTYWSLDPASQ----DMFDNGSFLRRRKRFKR 205
FOXD4L3 106 PAKPPYSYIALITMAILQNPHKRLTLSGICAFISGRFPYYRR-----KFPAWQNSIRHNLSLNDCFVKIPREPGHP----GKGNYWSLDPASQ----DMFDNGSFLRRRKRFKR 206
FOXD4L4 106 PAKPPYSYIALITMAILQNPHKRLTLSGICAFISGRFPYYRR-----KFPAWQNSIRHNLSLNDCFVKIPREPGHP----GKGNYWSLDPASQ----DMFDNGSFLRRRKRFKR 206
FOXD4L5 106 PAKPPYSYIALITMAILQNPHKRLTLSGICAFISGRFPYYRR-----KFPAWQNSIRHNLSLNDCFVKIPREPGHP----GKGNYWSLDPASQ----DMFDNGSFLRRRKRFKR 206
FOXD4L6 106 PAKPPYSYIALITMAILQNPHKRLTLSGICAFISGRFPYYRR-----KFPAWQNSIRHNLSLNDCFVKIPREPGHP----GKGNYWSLDPASQ----DMFDNGSFLRRRKRFKR 206
FOXE1    51 RGKPPYSYIALIAMAIAHAPERRLTLGGIYKFITERFPFYRD-----NPKKWQNSIRHNLTLNDCFLKIPREAGRP----GKGNYWALDPNAE----DMFESGSFLRRRKRFKR 151
FOXE3    69 RGKPPYSYIALIAMALAHAPGRRLTLAAIYRFITERFAFYRD-----SPRKWQNSIRHNLTLNDCFVKVPREPGNP----GKGNYWTLDPAAA----DMFDNGSFLRRRKRFKR 169
FOXF1    46 PEKPPYSYIALIVMAIQSSPTKRLTLSEIYQFLQSRFPFFRG-----SYQGWKNSVRHNLSLNECFIKLPKGLGRP----GKGHYWTIDPASE----FMFEEGSFRRRPRGFRR 146
FOXF2    98 PEKPPYSYIALIVMAIQSSPSKRLTLSEIYQFLQARFPFFRG-----AYQGWKNSVRHNLSLNECFIKLPKGLGRP----GKGHYWTIDPASE----FMFEEGSFRRRPRGFRR 198
FOXG1   179 YEKPPFSYNALIMMAIRQSPEKRLTLNGIYEFIMKNFPYYRE-----NKQGWQNSIRHNLSLNKCFVKVPRHYDDP----GKGNYWMLDPSSD----DVFIGGTTGKLRRRSTT 279
FOXH1    31 HDKPPYTYLAMIALVIQAAPSRRLKLAQIIRQVQAVFPFFRE-----DYEGWKDSIRHNLSSNRCFRKVPKDPAKP---QAKGNFWAVDVSLIPAEALRLQNTALCRRWQNGGA 136
FOXI1   121 LVRPPYSYSALIAMAIHGAPDKRLTLSQIYQYVADNFPFYNK-----SKAGWQNSIRHNLSLNDCFKKVPRDEDDP----GKGNYWTLDPNCE----KMFDNGNFRRKRKRKSD 221
FOXI2   100 LVRPPYSYSALIAMAIQSAPLRKLTLSQIYQYVAGNFPFYKR-----SKAGWQNSIRHNLSLNDCFKKVPRDEDDP----GKGNYWTLDPNCE----KMFDNGNFRRKRKRRAE 200
FOXI3   143 MVRPPYSYSALIAMAIQSAPERKLTLSHIYQFVADSFPFYQR-----SKAGWQNSIRHNLSLNDCFKKVPRDEDDP----GKGNYWTLDPNCE----KMFDNGNFRRKRKRRSE 243
FOXJ1   119 HVKPPYSYATLICMAMQASKATKITLSAIYKWITDNFCYFRH-----ADPTWQNSIRHNLSLNKCFIKVPREKDEP----GKGGFWRIDPQYA----ERLLSGAFKKRRLPPVH 219
FOXJ2    64 DGKPRYSYATLITYAINSSPAKKMTLSEIYRWICDNFPYYKN-----AGIGWKNSIRHNLSLNKCFRKVPRPRDDP----GKGSYWTIDTCPD----ISRKRRHPPDDDLSQDS 164
FOXJ3    76 DGKPPYSYASLITFAINSSPKKKMTLSEIYQWICDNFPYYRE-----AGSGWKNSIRHNLSLNKCFLKVPRSKDDP----GKGSYWAIDTNPK----EDVLPTRPKKRARSVER 176
FOXK1   303 ESKPPFSYAQLIVQAISSAQDRQLTLSGIYAHITKHYPYYRT-----ADKGWQNSIRHNLSLNRYFIKVPRSQEEP----GKGSFWRIDPASE----AKLVEQAFRKRRQRGVS 403
FOXK2   256 DSKPPYSYAQLIVQAITMAPDKQLTLNGIYTHITKNYPYYRT-----ADKGWQNSIRHNLSLNRYFIKVPRSQEEP----GKGSFWRIDPASE----SKLIEQAFRKRRPRGVP 356
FOXL1    47 PQKPPYSYIALIAMAIQDAPEQRVTLNGIYQFIMDRFPFYHD-----NRQGWQNSIRHNLSLNDCFVKVPREKGRP----GKGSYWTLDPRCL----DMFENGNYRRRKRKPKP 147
FOXL2    52 AQKPPYSYVALIAMAIRESAEKRLTLSGIYQYIIAKFPFYEK-----NKKGWQNSIRHNLSLNECFIKVPREGGGE----RKGNYWTLDPACE----DMFEKGNYRRRRRMKRP 152
FOXM1   234 SERPPYSYMAMIQFAINSTERKRMTLKDIYTWIEDHFPYFKHI----AKPGWKNSIRHNLSLHDMFVRETS---AN----GKVSFWTIHPSANRYL---TLDQVFKPL------ 327
FOXN1   269 FPKPIYSYSILIFMALKNSKTGSLPVSEIYNFMTEHFPYFKT-----APDGWKNSVRHNLSLNKCFEKVENKSGSS---SRKGCLWALNPAKIDKMQEELQKWKRKDPIAVRKS 374
FOXN2   110 TSKPPYSFSLLIYMAIEHSPNKCLPVKEIYSWILDHFPYFAT-----APTGWKNSVRHNLSLNKCFQKVERSHGKV---NGKGSLWCVDPEYKPNLIQALKKQPFSSASSQNGS 215
FOXN3   112 NCKPPYSFSCLIFMAIEDSPTKRLPVKDIYNWILEHFPYFAN-----APTGWKNSVRHNLSLNKCFKKVDKERSQS---IGKGSLWCIDPEYRQNLIQALKKTPYHPHPHVFNT 217
FOXN4   191 YPKPIYSYSCLIAMALKNSKTGSLPVSEIYSFMKEHFPYFKT-----APDGWKNSVRHNLSLNKCFEKVENKMSGS---SRKGCLWALNLARIDKMEEEMHKWKRKDLAAIHRS 296
FOXO1   158 NAWGNLSYADLITKAIESSAEKRLTLSQIYEWMVKSVPYFKDKGDSNSSAGWKNSIRHNLSLHSKFIRVQNE---G---TGKSSWWMLNPEGGK-------SGKSPRRRAASMD 258
FOXO3   155 NAWGNLSYADLITRAIESSPDKRLTLSQIYEWMVRCVPYFKDKGDSNSSAGWKNSIRHNLSLHSRFMRVQNE---G---TGKSSWWIINPDGGK-------SGKAPRRRAVSMD 255
FOXO4    99 NAWGNQSYAELISQAIESAPEKRLTLAQIYEWMVRTVPYFKDKGDSNSSAGWKNSIRHNLSLHSKFIKVHNE---A---TGKSSWWMLNPEGGK-------SGKAPRRRAASMD 199
FOXO6    86 NAWGNLSYADLITKAIESAPDKRLTLSQIYDWMVRYVPYFKDKGDSNSSAGWKNSIRHNLSLHTRFIRVQNE---G---TGKSSWWMLNPEGGK-------TGKTPRRRAVSMD 186
FOXP1   463 EVRPPFTYASLIRQAILESPEKQLTLNEIYNWFTRMFAYFRR-----NAATWKNAVRHNLSLHKCFVRVEN---------VKGAVWTVDEVEF-----------QKRRPQKIS 550
FOXP2   502 DVRPPFTYATLIRQAIMESSDRQLTLNEIYSWFTRTFAYFRR-----NAATWKNAVRHNLSLHKCFVRVEN---------VKGAVWTVDEVEY-----------QKRRSQKIT 589
FOXP3   335 NMRPPFTYATLIRWAILEAPEKQRTLNEIYHWFTRMFAFFRN-----HPATWKNAIRHNLSLHKCFVRVES---------EKGAVWTVDELEF-----------RKKRSQRPS 422
FOXP4   465 DVRPPFTYASLIRQAILETPDRQLTLNEIYNWFTRMFAYFRR-----NTATWKNAVRHNLSLHKCFVRVEN---------VKGAVWTVDEREY-----------QKRRPPKMT 552
FOXQ1   117 RPKPPYSYIALIAMAIRDSAGGRLTLAEINEYLMGKFPFFRG-----SYTGWRNSVRHNLSLNDCFVKVLRDPSRP---WGKDNYWMLNPNSE----YTFADGVFRRRRKRLSH 218
FOXR1   171 WSRPPLNYFHLIALALRNSSPCGLNVQQIYSFTRKHFPFFRT-----APEGWKNTVRHNLCFRDSFEKVPVSMQGGASTRPRSCLWKLTEEGHRRFAEEARALASTRLESIQQC 279
FOXR2   190 WQRPPLNCSHLIALALRNNPHCGLSVQEIYNFTRQHFPFFWT-----APDGWKSTIHYNLCFLDSFEKVPDSLKDEDNARPRSCLWKLTKEGHRRFWEETRVLAFAQRERIQEC 298
FOXS1    16 PTKPPYSYIALIAMAIQSSPGQRATLSGIYRYIMGRFAFYRH-----NRPGWQNSIRHNLSLNECFVKVPRDDRKP----GKGSYWTLDPDCH----DMFEHGSFLRRRRFTR 116
```

**Figure S2.**

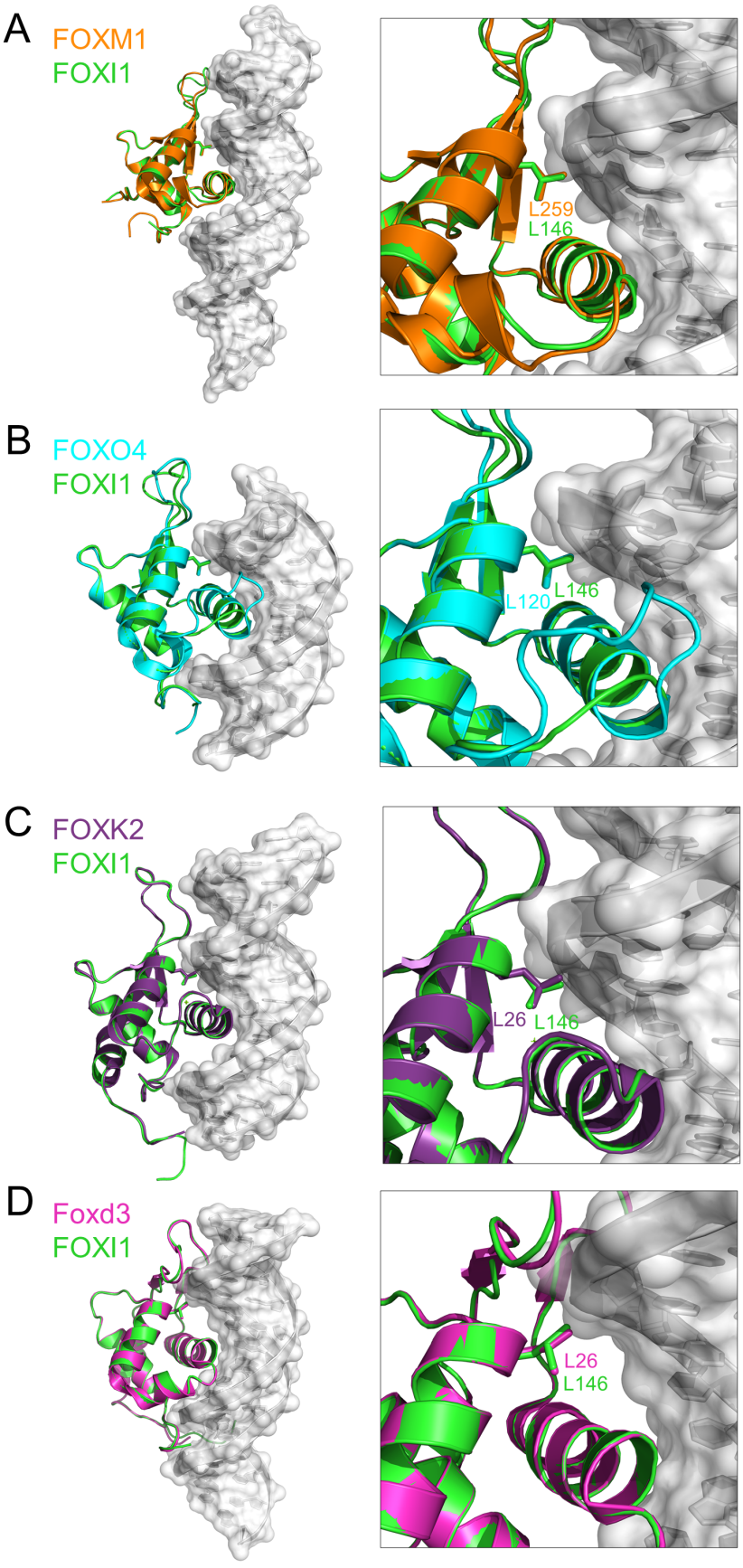
A
FOXM1
FOXI1
L259
L146
B
FOXO4
FOXI1
L120
L146
C
FOXK2
FOXI1
L26
L146
D
Foxd3
FOXI1
L26
L146

**Figure S3.**

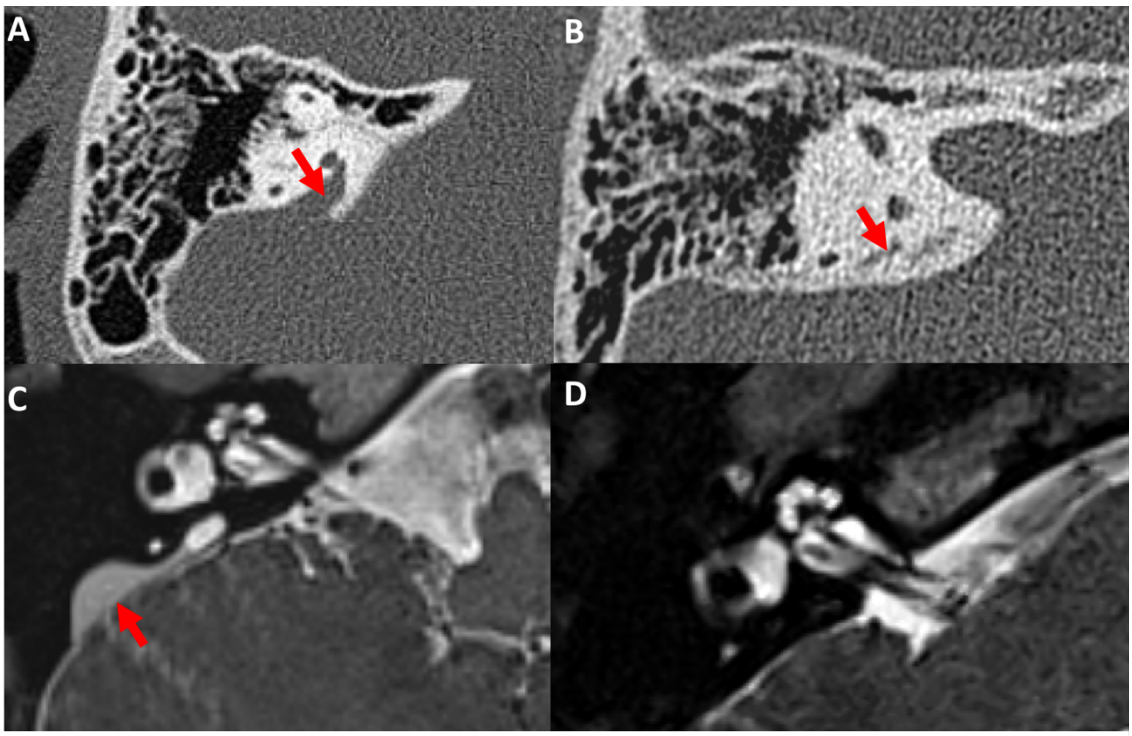


**Figure S4.**

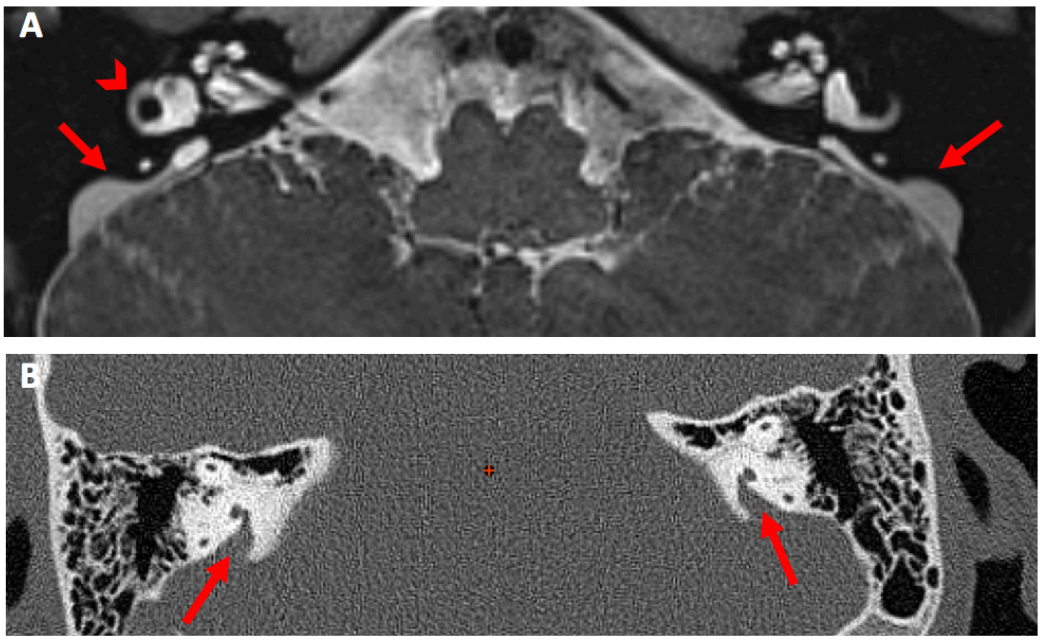

**Figure S5.**

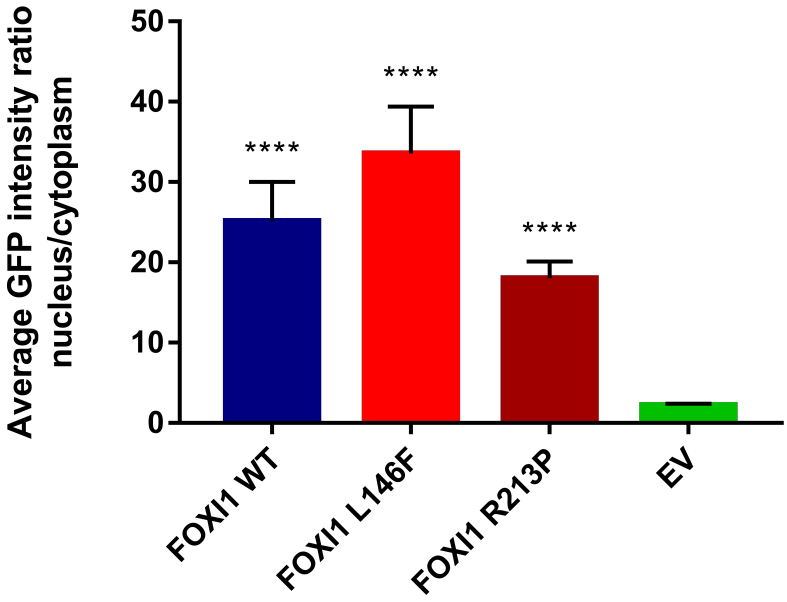


**Figure S6.**

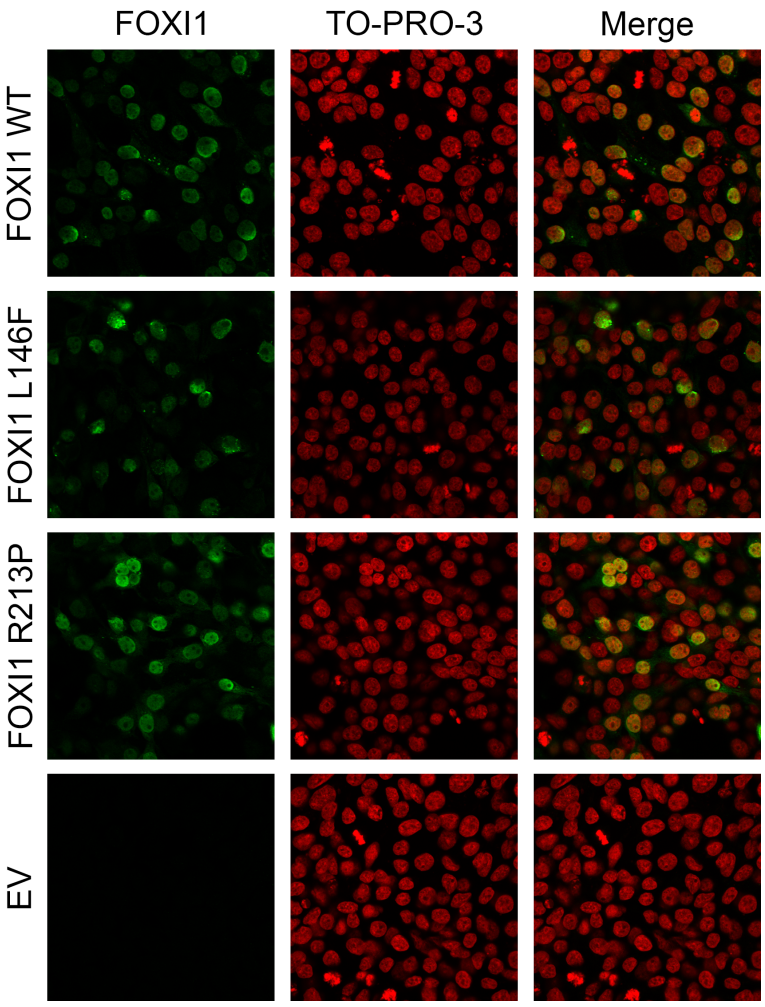

ACKNOWLEDGEMENTS

We thank the patients and their family members for their help in this study. JAS is funded by the Medical Research Council (MR/M012212/1), Kidney Research UK, Kids Kidney Research, Northern Counties Kidney Research Fund and the Newcastle upon Tyne Hospitals NHS Charity. Funding for this study to RK, DB was kindly provided by the European Union, FP7 (grant agreement 2012-305608 “European Consortium for High-Throughput Research in Rare Kidney Diseases (EURenOmics)”) and Kids Kidney research, Kidney Research UK and The John Moorhead Trust. SE is supported by the Swedish Research Council (2014–2516), The Knut and Alice Wallenberg Foundation, Sahlgrenska's University Hospital (LUA-ALF), The Inga Britt and Arne Lundgren Foundation, The Torsten Söderberg Foundation, Novo Nordisk Foundation, and The King Gustaf V and Queen Victoria Freemason Foundation. CAW is supported by the Swiss National Science Foundation (155959 and NCCR Kidney.CH) and the European Union FP7 project EURenOmics.

## SUPPLEMENTARY FIGURE LEGENDS

**Figure S1.** Panel A shows the crystal structure of FOXM1 (PBD accession code 3G73)[4] colored from N-terminal (blue) to C-terminal (red) domains. Secondary structural elements are labelled: α-helices (α1-α3); β-sheets (β1-β3); and wing domains 1 and 2 (W1 and W2, respectively). Panel B shows a cartoon representation of the FOXM1 DNA-binding domain (colored as in A), depicting the approximate position of the structural elements within human FOX proteins (sequences aligned below). The position of FOXI1 L146 in α2 and FOXI1 R213 in W2 are highlighted by red and black arrows, respectively.

**Figure S2.** Homology modelling results for FOXI1 (in green) consistently identified FOXI1 L146 as occupying an identical position to functionally important leucine residues (numbered as in the reports) in the structures of FOXM1 (panel A, in orange; PDB code 3G73), FOXO4 (panel B, in cyan; PDB code 3L2C), FOXK2 (panel C, in purple; PDB code 2C6Y) and Foxd3 (panel D, in magenta; PDB code 2HDC). Note that the region of the wing 2 domain (W2) wherein FOXI1 R213 resides was not either not resolved in these structures (FOXM1 and FOXO4) or was not captured interacting with the target DNA (FOXK2 and Foxd3).

**Figure S3.** Dilatation of the vestibular aqueduct and the endolymphatic sac contained within. Shown are images of the inner ear of patient 2.1 (Panel A and C in comparison to a normal control (Panel B and D). A: High resolution CT of the petrous bones shows enlargement of the vestibular aqueduct (arrow). B. The normal vestibular aqueduct is barely visible as a small linear hypodensity (arrow). C: High resolution NMR (T2) shows dilatation of the endolymphatic sac (arrow). D: The endolymphatic sac is not visible on the NMR in the control due to its small size.

**Figure S4.** A: High resolution NMR (T2) shows symmetrical dilatation of the endolymphatic sac (arrows). Note that the signal of the fluid in the sacs is slightly hypointense to the signal in the lateral semicircular canals (arrowhead), due to high proteinaceous content. B: High resolution CT of the petrous bones shows corresponding enlargement of the vestibular aqueduct (arrows).

**Figure S5.** Determination of nuclear versus cytoplasmic GFP in 293 cells. Using ImageJ, the ratio of average GFP signal intensity in the nucleus to the average intensity in the cytoplasm of cells, (n=15 per condition), was calculated based on square-shaped equally sized regions of interest (ROIs). The results show that the ratio, considered a measure of the amount of GFP in the nucleus, was similarly and significantly higher for all three FOXI1-GFP constructs compared to the empty pEGFP-N3 plasmid (EV) (**** $p < 0.0001$). This indicates that the loss of activation of FOXI1 target genes by the two mutations is not caused by a redistribution of the FOXI1 protein. Error bars, ±sem.

**Figure S6.** Immunofluorescent staining of FOXI1 transfected 293 cells. 293 cells were transiently transfected with pcDNA3.1 expression plasmid carrying wild-type FOXI1 or either of the two mutated FOXI1 variants. Empty pcDNA3.1 was used as empty vector control (EV). Immunofluorescent staining with anti-FOXI1 antibody (Abcam, ab20454) showed that FOXI1 in all cases was primarily localized to the nucleus. No endogenous FOXI1 protein could be detected in empty vector control (EV). To-PRO-3 stains nuclei.

## REFERENCES


1. Clark KL, Halay ED, Lai E, Burley SK. Co-crystal structure of the HNF-3/fork head DNA-recognition motif resembles histone H5. Nature 1993;364:412-20.
2. Soding J. Protein homology detection by HMM-HMM comparison. Bioinformatics 2005;21:951-60.
3. Sali A, Blundell TL. Comparative protein modelling by satisfaction of spatial restraints. Journal of molecular biology 1993;234:779-815.
4. Littler DR, Alvarez-Fernandez M, Stein A, et al. Structure of the FoxM1 DNA-recognition domain bound to a promoter sequence. Nucleic acids research 2010;38:4527-38.
5. Boura E, Rezabkova L, Brynda J, Obsilova V, Obsil T. Structure of the human FOXO4-DBD-DNA complex at 1.9 A resolution reveals new details of FOXO binding to the DNA. Acta crystallographica Section D, Biological crystallography 2010;66:1351-7.
6. Tsai KL, Huang CY, Chang CH, Sun YJ, Chuang WJ, Hsiao CD. Crystal structure of the human FOXK1a-DNA complex and its implications on the diverse binding specificity of winged helix/forkhead proteins. The Journal of biological chemistry 2006;281:17400-9.
7. Jin C, Marsden I, Chen X, Liao X. Dynamic DNA contacts observed in the NMR structure of winged helix protein-DNA complex. Journal of molecular biology 1999;289:683-90.
8. Murphy TC, Saleem RA, Footz T, Ritch R, McGillivray B, Walter MA. The wing 2 region of the FOXC1 forkhead domain is necessary for normal DNA-binding and transactivation functions. Invest Ophthalmol Vis Sci 2004;45:2531-8.
9. Blomqvist SR, Vidarsson H, Fitzgerald S, et al. Distal renal tubular acidosis in mice that lack the forkhead transcription factor Foxi1. The Journal of clinical investigation 2004;113:1560-70.
10. Vidarsson H, Westergren R, Heglind M, Blomqvist SR, Breton S, Enerback S. The forkhead transcription factor Foxi1 is a master regulator of vacuolar H-ATPase proton pump subunits in the inner ear, kidney and epididymis. PloS one 2009;4:e4471.
11. Blomqvist SR, Vidarsson H, Soder O, Enerback S. Epididymal expression of the forkhead transcription factor Foxi1 is required for male fertility. The EMBO journal 2006;25:4131-41.